ELSEVIER   CrossMark

● *Original Contribution*

COMMON CAROTID ARTERY FLOW MEASURED BY 3-D ULTRASONIC VECTOR FLOW IMAGING AND VALIDATED WITH MAGNETIC RESONANCE IMAGING

Simon Holbek,[*] Kristoffer Lindskov Hansen,[†] Hamed Bouzari,[*] Caroline Ewertsen,[†]
Matthias Bo Stuart,[*] Carsten Thomsen,[†] Michael Bachmann Nielsen,[†]
and Jørgen Arendt Jensen[*]

[*] Center for Fast Ultrasound Imaging, Department of Electrical Engineering, Technical University of Denmark, Lyngby,
Denmark; and [†] Department of Radiology, Copenhagen University Hospital, Rigshospitalet, Copenhagen, Denmark

Abstract—Ultrasound (US) examination of the common carotid artery was compared with a through-plane magnetic resonance imaging (MRI) sequence to validate a recently proposed technique for 3-D US vector flow imaging. Data from the first volunteer examined were used as the training set, before volume flow and peak velocities were calculated for the remaining eight volunteers. Peak systolic velocities (PSVs) and volume flow obtained with 3-D US were, on average, 34% higher and 24% lower than those obtained with MRI, respectively. A high correlation was observed for PSV ($r = 0.79$), whereas a lower correlation was observed for volume flow ($r = 0.43$). The overall standard deviations were ±5.7% and ±5.7% for volume flow and PSV with 3-D US, compared with ±2.7% and ±3.2% for MRI. Finally, the data were re-processed with a change in the parameter settings for the echo-canceling filter to investigate its influence on overall performance. PSV was less affected by the re-processing, whereas the difference in volume flow between 3-D vector flow imaging and MRI was reduced to −9%, and with an improved overall standard deviation of ±4.7%. The results illustrate the feasibility of using 3-D US for precise and angle-independent volume flow and PSV estimation *in vivo*. (E-mail: sholbek@elektro.dtu.dk)   © 2017 World Federation for Ultrasound in Medicine & Biology.

Key Words: Vector flow imaging, Transverse oscillation, 3-Dimensional, Blood flow quantification, Magnetic resonance imaging, Volume flow.

INTRODUCTION

Pathology in the vessels is often reflected directly in the related hemodynamics. For instance, increased blood velocity is observed in stenotic vessels (Alexandrov et al. 1997; Phillips et al. 1980), and the change in volume flow in patients with arteriovenous fistulas is used to monitor the risk of developing a stenosis (Whittier 2009; Wiese and Nonnast-Daniel 2004). Ultrasound (US) is an easily accessible imaging modality that can provide the required information in real time. Currently, 1-D Doppler techniques and 2-D vector flow imaging (VFI) techniques can be used to estimate both velocities and volume flow, and have been applied clinically (Brandt et al. 2016). In this article, *D* refers to the dimension of known velocity components mapped on a 2-D image. The exception is 1-D spectral Doppler ultrasound

(SDUS), which provides 1-D velocity information in a single point.

One-dimensional US methods, however, are subject to errors in velocity estimation because of, for example, geometric spectral broadening, which depends on the transducer dimension and relative examination location (Hoskins et al. 1999) and angle dependency (Picot and Embree 1994). The angle dependency encountered in 1-D US requires an operator to manually compensate for the flow direction and to assume that the out-of-plane velocity component is insignificant. It also assumes a fixed angle throughout the cardiac cycle, which is generally incorrect (Udesen et al. 2008). For 2-D vector flow methods (Bohs and Trahey 1991; Fadnes et al. 2015; Jensen 2001; Lenge et al. 2015; Nikolov and Jensen 2003; Udesen et al. 2008; Villagomez-Hoyos et al. 2016b; Yiu et al. 2014), angle dependency has been solved, but still relies on the assumption that the out-of-plane velocity component does not contribute to the flow.

Address correspondence to: Simon Holbek, Ørsteds Plads, Building 349, 2800 Kgs Lyngby, Denmark. E-mail: sholbek@elektro.dtu.dk

Volumetric flow rates can be estimated with either 1-D Doppler techniques (Struijk et al. 2005) or 2-D vector flow techniques (Hansen et al. 2017). Both types of techniques rely on several operator decisions and necessary mathematical assumptions about flow and vessel geometry symmetry, which influence the accuracy of the estimates (Jensen et al. 2016). These decisions and assumptions are significantly reduced for 3-D US VFI techniques, for which there are a variety of approaches (Correia et al. 2016; Holbek et al. 2016, 2017; Pihl and Jensen 2014; Pihl et al. 2014; Provost et al. 2014; Villagomez-Hoyos et al. 2016a; Wigen and Løvstakken 2016).

The purpose of the work described here was to determine the accuracy of the angle-independent 3-D US method proposed in previous work (Holbek et al. 2017) for accurate flow quantification. The method is validated in a clinical setup by scanning the common carotid artery (CCA) in nine healthy volunteers and comparing the results with magnetic resonance imaging (MRI) results. Several studies have compared MRI with US (Harloff et al. 2009, 2013; Hansen et al. 2009); however, this work presents the first comparison of 3-D VFI with MRI.

METHODS

Three measurements were performed in each volunteer: two US measurements (SDUS and 3-D US) and one MRI measurement. The US and the MRI examinations were conducted by two clinicians (K.L.H. and C.E), each with more than 10 years of experience in radiology.

Volunteers

Nine healthy volunteers were included in this study. The study was performed after approval by the Danish National Committee on Biomedical Research Ethics (H-1-2014-FSP-072), and written informed consent was obtained from all volunteers.

Two women and 7 men ranging in age from 27 to 52 y (median 30) and ranging in body mass index from 20 to 27 kg/m^2 (mean 24 $\pm$ 2.7 kg/m^2) were included in the study.

Experimental procedure

All volunteers fasted for at least 2 h and rested in the supine position for 15 min before all examinations. The right CCA was examined in all volunteer using 1-D SDUS, 3-D US and MRI. Data were acquired on 2 consecutive days for each volunteer. On day 1, the 3-D US measurement was conducted, and on day 2, the MRI examination was performed. The examinations were carried out on two different days, as the experimental scanner used for 3-D US and the MRI scanner were permanently installed at different locations.

After each 3-D US acquisition, a maximum of 0.5 s of data was processed and inspected to ensure that data were not corrupted. The only exception to this were data from volunteer 1, which were used as the training sample to lock all the various parameters in the post-processing stage. Data from the remaining eight volunteers were processed according to the training sample. This was first done after the last volunteer had completed both the MRI examination and the 3-D US measurement.

Spectral Doppler measurements

A reference measurement with SDUS was made prior to both the 3-D US measurement and MRI examination. The reference measurement consisted of an approximately 10-s cine loop with SDUS velocity information, recorded 2–3 cm upstream of the bifurcation in the common carotid artery. A 5.2–MHz linear array transducer (9032, BK Ultrasound, Herlev, Denmark) and a commercial scanner (BK 5000, BK Ultrasound) were used for these measurements.

The SDUS cine loop for each volunteer was stored and processed offline. The entire cine loop was evaluated, and the peak velocities displayed were manually noted for each of the recorded heart cycles, from which the mean values and standard deviations were calculated.

3-D US measurements

Three-dimensional US measurements were performed in an experimental laboratory, where a 2-D 32 × 32-element phased array transducer with a center frequency of 3.5 MHz was used (Vermon S.A., Tours, France). The transducer was connected to the experimental ultrasound scanner SARUS (Jensen et al. 2013), which sampled from all 1024 channels at a sampling frequency of 17.5 MHz.

An interleaved flow and B-mode emission sequence described in previous work was used (Holbek et al. 2017). The flow sequence contained focused steered emission and had a field-of-view of 30°, whereas the B-mode emissions consisted of diverging waves, which provided a 60° × 60° field-of-view volume using synthetic aperture imaging techniques. The transverse oscillation (TO) method (Jensen 2001; Jensen and Munk 1998) was used for velocity estimation. The pulse repetition frequency (f_{prf}) was 12.6 kHz. Intensities of the applied 3-D US sequence were as follows: mechanical index (MI) = 1.14, and $I_{spta.3}$ = 439 mW/cm^2, which are below U.S. Food and Drug Administration limits (FDA 2008). A total of 7.5 s of data were recorded for each measurement and stored offline for further processing.

3-D US data analysis

Processing of the 3-D US data was identical to the procedure described in previous work (Holbek et al.

2017). A manual segmentation of the individual vessel lumen was performed by K.L.H. based on a B-mode image. The segmentation task was performed using a graphical user interface that allowed the clinician to draw a mask as desired. The clinician was blinded to the performance of the drawn mask. Only estimated 3-D velocities within the drawn masks were used in further analysis. The final outcome of the processing was a scan converted and interpolated 2-D velocity map for all three velocity components (v_x, v_y, v_z) at every sampled time. The applied 3-D US sequence provided 1145 velocity estimates per second. Temporal flow rates $Q(t)$ were calculated for every frame as the mean of the velocity component perpendicular to the scan plane multiplied by the area of the drawn mask. Peak velocities were similarly calculated for every frame at every pixel location $v(x, y)$ within the mask as

$$v(x, y, t) = \sqrt{v_x(x, y, t)^2 + v_y(x, y, t)^2 + v_z(x, y, t)^2} \quad (1)$$

The maximum value of $v(x, y, t)$ within a circular range gate of 2 mm in the center of the vessel was used as the peak velocity in future calculations and statistics.

MRI measurements

A 1.5-T whole-body scanner (Avanti, Siemens, Erlangen, Germany) with a head and neck matrix coil was used for the MRI examination. Initially, an anatomical time-of-flight sequence was performed on the volunteer to identify the location of the CCA. Based on the anatomical image, a plane was selected perpendicular to the CCA and located 2–3 cm before the bifurcation. The MRI scan plane was selected by the clinician to yield a distance approximately similar to that for the bifurcation, as for the 3-D US scan plane. Within this plane, a retrospective electrocardiography-gated phase contrast sequence was used to estimate through-plane velocities. The sequence had a repetition time of 42 ms, echo time of 3 ms, flip angle of 20°, pixel resolution of 1.1 mm × 1.1 mm in an image of size 216 × 256 and a slice thickness of 5 mm. The maximum velocity encoding was patient specific and adjusted manually by the operators to avoid aliasing. The range of the velocity encoding spanned from ±100 to ±130 cm/s. The total number of phases per heartbeat was fixed at 50. MRI velocity measurements were repeated three times in a row, and all three data sets were stored and included in the analysis. Each data set was acquired in the period of 210 heart cycles.

MRI data analysis

The stored MRI DICOM data were processed offline using MATLAB (The MathWorks, Natick, MA, USA) by adding the 50 temporal frames to create an anatomical grayscale intensity map with the purpose of suppressing noise and enhancing vessel regions. The intensity map was subsequently converted to a binary image by applying a manually selected threshold of the maximum intensity to segment out vessel regions. The threshold was adjusted for every data set and for every volunteer. Morphological operations as described in previous work (Holbek et al. 2017) were applied to the binary image to identify all potential vessels. Finally, the vessel region encapsulating the right CCA was selected manually, and only flow estimates within this mask and the area of the mask were used in the analysis.

Comparison between MRI and 3-D US

Data from the MRI examination were electrocardiography gated and provided the mean velocities throughout the heart cycle, whereas 3-D US provided continuous velocity estimates over several heart cycles with a starting point anywhere in the cardiac cycle. Furthermore, there were physiological variations in the heart cycle duration between the MRI and the 3-D US examinations because data were not acquired simultaneously. For a comparison between MRI and 3-D US, the two data sets had to be aligned to the same starting point in the heart cycle; moreover, the evaluation period had to be the same for MRI and 3-D US.

To comply with MRI data, an automatic autocorrelation routine was applied to the temporal flow rate estimates $Q(t)$ obtained with 3-D US with the purpose of dividing and aligning all captured heart cycles. The aligned heart cycles all started during the end-diastolic phase, similar to the MRI data. Because of physiological variation in each heartbeat, only 90% of the mean cycle length was kept, meaning that data from the late diastolic phase were discarded in the 3-D US data set.

On the basis of data from the respective aligned heart cycles, the mean cycle flow rate and mean cycle peak velocity were calculated for all volunteers. Moreover, the standard deviation (SD) was calculated based on the aligned cycles. Aligned volume flow with similar truncated heart cycle lengths was chosen as the flow rate comparison metric, as this ensured a similar observation time window with the same offset in the heart cycle for both MRI and 3-D US. Moreover, calculating the volume flow as milliliters per stroke instead of milliliters per second provides a metric that is less affected by the heart cycle duration (Higginbotham et al. 1986). Mean volume flow were averaged from $t = 0$ in the aligned heart cycle to $t = t_{min}$, where t_{min} was the shortest estimated stroke time between MRI and 3-D US. The stroke time could therefore vary between volunteers and could be dictated by either MRI or 3-D US.

Bland–Altman plots along with confidence intervals were computed using a Kolmogorov–Smirnov test to illustrate differences between and similarities in MRI,

3-D US and the reference spectral Doppler ultrasound measurements (Bland and Altman 1986). The comparison between MRI and 3-D US was made for estimated mean volume flow, peak systolic velocity (PSV) and end-diastolic velocity (DV). Correlations of selected variables were estimated with Pearson's correlation coefficient using MATLAB.

Changing the echo-canceling filter

The applied echo-canceling was optimized for the training set, where a fixed amplitude threshold value of 8000 was used as a parameter in the energy-based frequency cutoff filter (Villagomez-Hoyos 2016). The filter was therefore not designed to adapt to the initial clutter level, which was expected to vary between volunteers because of physiological variations. The purpose of such a filter is to cancel out stationary echoes from vessel surroundings (Friemel et al. 1993). It was anticipated that in cases where the threshold was set too high relative to the present circumstances, a large fraction of signal originating from clutter would pass the filter. On the other hand, if the threshold was set too low compared with the given environment, the echo-canceling filter would remove energy both from the stationary tissue and from the scattered blood cell signal. Neither case is optimal and will lead either to an underestimation if the threshold is too high because the velocity estimates would be highly influenced by the surrounding tissue movement, or to imprecise estimates if the selected threshold is too low, as the signal would be dominated by noise.

To investigate if the echo-canceling filter was selected properly, the data were subsequently reprocessed with a modified echo-canceling amplitude threshold. The modified threshold level was selected retrospectively. All remaining processing parameters were kept fixed according to the training samples.

RESULTS

Performance of the training set

The performance of the training set (volunteer 1) between MRI- and 3-D US–derived flow rates and peak velocities is illustrated in Figure 1. The mean PSV estimated with 3-D US was 97.3 ± 6.3 cm/s, compared with 77.3 ± 1.2 cm/estimated with MRI, which is a 26% overestimation (Table 1). The mean flow rate across the cycle was 6.6 ± 0.6 mL/stroke for 3-D US, which was 20.0% lower than the 8.3 ± 0.1 mL/stroke estimated with MRI. Overall, a close correspondence was observed between the waveforms throughout the cycle.

Correlation between MRI and US measurements

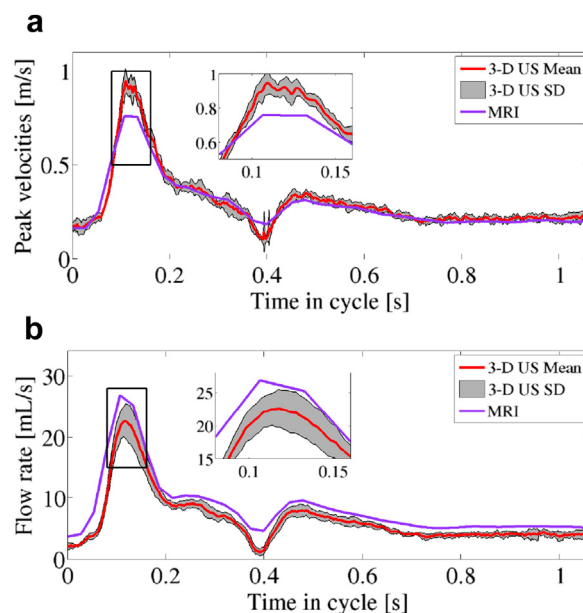The mean reference PSV obtained with SDUS techniques prior to the MRI and 3-D US measurements

Fig. 1. Coherently aligned mean cycle quantities estimated with 3-D ultrasound (US) (*red curve*) ± one standard deviation (*gray area*) along with the similar quantity found with magnetic resonance imaging (MRI) (*purple curve*). The data are (a) peak velocities and (b) flow rates for the training set (volunteer 1). SD = standard deviation.

were 99 ± 28 and 100 ± 23 cm/s, which indicated that hemodynamic conditions in MRI and 3-D US are similar. However, the statistical comparison between mean peak velocities obtained with SDUS and 3-D US or MRI reveals high agreement between SDUS and 3-D US ($p = 0.49$) (Table 1), but much lower agreement between SDUS and MRI ($p < 0.01$) (Fig. 2a). In general, MRI PSV was lower by 6%– 46% compared with SDUS PSV, whereas 3-D US peak velocities were in the range −25% to 26% compared with SDUS. A significant overestimation of the PSV for 3-D US compared with MRI ($p < 0.01$) was seen for all except one volunteer (Fig. 2b), whereas there was closer agreement between the DV values ($p = 0.022$) (Fig. 2c).

Volume flow estimated with 3-D US was in all but one case lower than the similar estimate obtained with MRI (Fig. 2d and Table 1). On average, 3-D US estimated 24% lower mean volume flow compared with MRI, for a poor correlation ($r = 0.43$). For PSV, 3-D US-derived estimates were 34% higher on average than MRI estimates, and a high correlation was seen ($r = 0.79$). In both cases, the overall SD for MRI were lower than those for 3-D US (2.7% and 3.2% compared with 5.7% and 5.7% for volume flow and PSV, respectively). DVs were on average underestimated by 5.2% with 3-D US compared with MRI, but were highly correlated ($r = 0.79$), similar to PSV.

Table 1. Estimated flow rates and peak systolic velocities for all nine volunteers*

No.	Stroke volume (mL/stroke)			PSV (cm/s)			DV (cm/s)		
	MRI	3-D US	3-D US new filter	MRI	3-D US	3-D US new filter	MRI	3-D US	3-D US new filter
1	8.3 ± 0.8%	6.6 ± 9.1%	9.0 ± 1.6%	77.3 ± 1.5%	97.3 ± 6.3%	113.3 ± 5.2%	16.2 ± 2.9%	18.0 ± 9.4%	21.4 ± 19.8%
2	5.8 ± 1.4%	4.6 ± 9.9%	5.7 ± 7.8%	61.6 ± 0.5%	69.5 ± 5.1%	76.3 ± 5.6%	21.0 ± 1.7%	17.2 ± 15.0%	19.1 ± 12.2%
3	9.2 ± 2.0%	5.0 ± 5.7%	5.5 ± 5.1%	83.5 ± 2.3%	122.5 ± 2.0%	128.4 ± 3.0%	26.3 ± 3.5%	26.3 ± 8.7%	29.5 ± 11.5%
4	6.8 ± 2.4%	2.9 ± 1.7%	5.8 ± 9.1%	46.4 ± 1.1%	44.0 ± 8.0%	64.4 ± 3.2%	15.4 ± 2.0%	11.6 ± 10.2%	19.1 ± 13.1%
5	6.0 ± 5.1%	6.2 ± 3.9%	6.4 ± 4.7%	65.0 ± 1.0%	116.7 ± 7.3%	91.2 ± 5.5%	14.7 ± 5.1%	14.9 ± 23.9%	12.1 ± 8.6%
6	7.3 ± 4.4%	6.9 ± 5.4%	7.7 ± 5.5%	87.6 ± 5.1%	101.9 ± 7.5%	105.0 ± 4.9%	18.0 ± 4.8%	19.9 ± 6.8%	19.1 ± 8.7%
7	8.6 ± 3.4%	7.1 ± 2.1%	6.7 ± 2.3%	73.5 ± 3.7%	93.4 ± 2.4%	90.3 ± 3.3%	19.8 ± 3.8%	19.7 ± 6.2%	20.4 ± 7.3%
8	9.2 ± 1.4%	7.1 ± 3.7%	7.6 ± 2.8%	75.6 ± 4.3%	114.9 ± 5.7%	110.4 ± 8.4%	19.1 ± 2.5%	18.5 ± 12.1%	15.2 ± 15.2%
9	6.2 ± 0.8%	5.3 ± 3.4%	6.7 ± 2.2%	51.9 ± 1.5%	76.3 ± 3.4%	88.2 ± 5.3%	21.8 ± 1.9%	16.9 ± 19.4%	23.1 ± 17.3%
Mean	7.5 ± 2.7%	5.7 ± 5.7%	6.8 ± 4.7%	69.2 ± 3.2%	92.9 ± 5.7%	96.4 ± 5.4%	19.1 ± 3.3%	18.1 ± 12.7%	19.9 ± 13.9%

MRI = magnetic resonance imaging; US = 3-D ultrasound; US new filter = 3-D US with new echo-canceling filter.
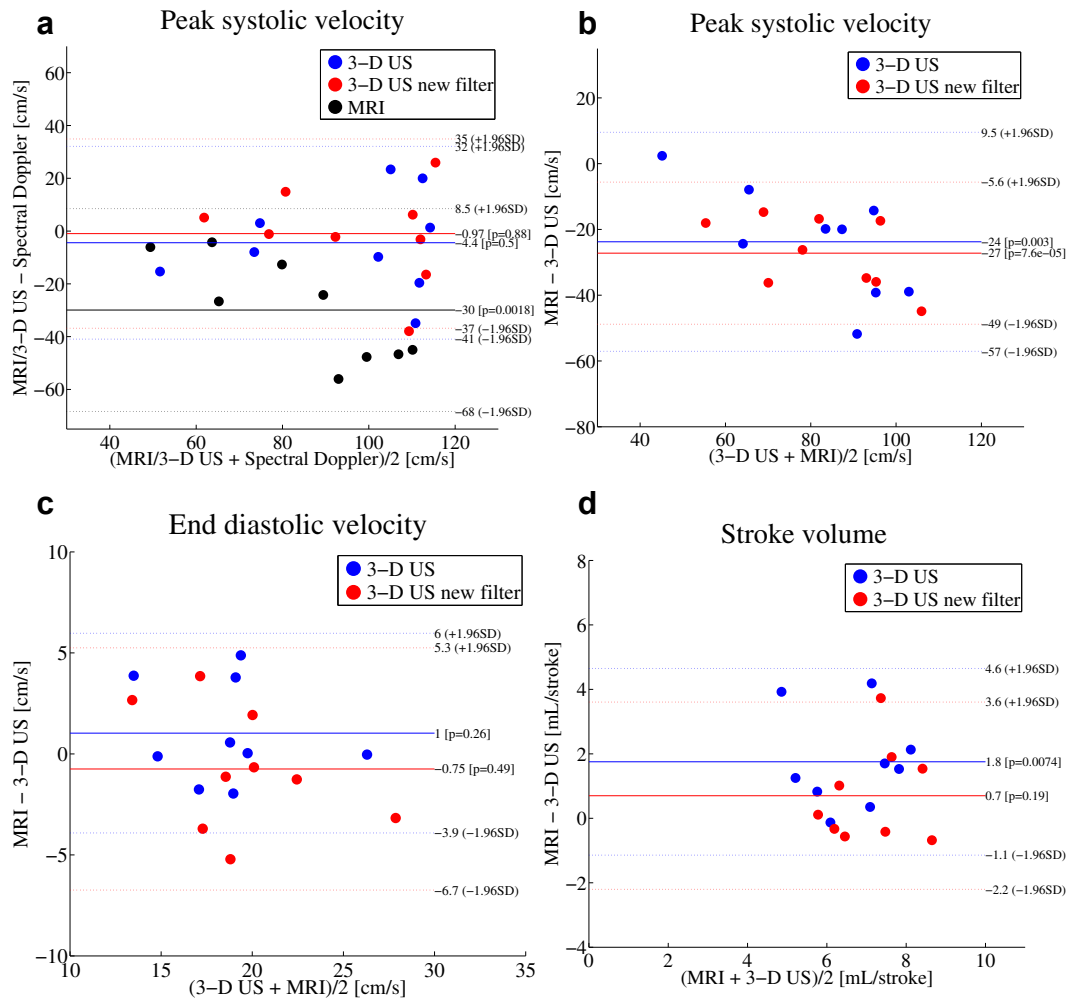* Values are means ± standard deviations.

Fig. 2. Bland–Altman plot with mean values ± 2 standard deviations for (a) reference spectral Doppler peak systolic velocities compared with MRI and 3-D US, (b) MRI systolic peak velocities compared with 3-D US, (c) MRI end-diastolic peak velocities compared with 3-D US, and (d) MRI volume flow compared with 3-D US. All figures are displayed both with the original choice of echo-canceling filter (*blue*) and with the new echo-canceling filter (*red*). Reference values are also shown in Table 2. US = ultrasound; MRI = magnetic resonance imaging; SD = standard deviation.

Influence of the echo-canceling filter

To test the influence of selecting the correct echo-canceling filter, data for all volunteers were re-processed with a modified threshold value. In a retrospective conclusion, the modified amplitude threshold was halved from 8000 to 4000. The re-processed data exhibited both a decrease in overall SD and an increase in overall mean volume flow to 6.8 mL/stroke. This narrowed the difference compared with MRI to an underestimation of 9%, although the correlation was poorer ($r = 0.31$) (Table 2). Furthermore, the overall mean PSV were almost unchanged and rose by 3% with only a minor change in the overall SD from $\pm 5.7\%$ to $\pm 5.4\%$. DV rose from an overall value of 18.1 to 19.9 cm/s, with a small increase in SD (Table 2). The correlation increased for PSV ($r = 0.84$), whereas for DV, the correlation was reduced slightly ($r = 0.78$.)

A 3-D vector representation of flow during the peak systole and end-diastolic phases is provided for volunteer 1 for both the initial and modified echo-canceling filters (Fig. 3). In this specific case, the PSV increased with the modified threshold, and a higher mean velocity was present without resulting in erroneous estimates.

DISCUSSION

The results described indicate that the proposed method for 3-D VFI with the initial echo-canceling filter provided a precision of less than $\pm 10\%$ (Table 1) for both volume flow and PSV in all nine volunteers, with an overall mean SD of 5.7% and 5.7%, respectively. These findings were similar for MRI, for which the overall mean SD were 2.7% and 3.2% for volume flow and PSV, respectively. The DV had higher overall SD of 12.7% for 3-D US and 3.6% for MRI compared with PSV.

The overestimation of PSV for US compared with MRI was in agreement with previous studies (Harloff et al. 2009, 2013). For flow rates obtained with 3-D US, a large underestimation by on average -24% compared with MRI was found. This difference contrasts with the overestimation in peak velocities throughout the majority

of the heart cycle. Furthermore, it is contrary to previous studies, in which similar flow rates were reported for MRI compared with a 3-D Doppler techniques in the mitral valve (Ge et al. 2005) and for various 2-D vector flow techniques in the common carotid artery (Hansen et al. 2009).

One explanation for the large underestimation in volume flow is that it was a consequence of the echo-canceling filter used in the 3-D US setup. Consequently, the threshold amplitude was reduced from 8000 to 4000, and data were re-processed. Lowering the threshold influenced the estimates by increasing the mean velocities for 3-D US without increasing the overall SD. Furthermore, PSV increased only slightly with this maneuver. When re-processing the data, the difference in overall volume flow between 3-D US and MRI was reduced from -24% to -9%. For accurate peak velocity estimations, the effect is less prominent compared with a volume flow examinations, where a large bias occurs if the areas close to the vessel wall are underestimating the velocities. These results highlight the importance of making the echo-canceling threshold adaptive and possibly also varying within the heart cycle; this should be the focus of future work.

Even though a large mean difference was found in the estimation of PSV between 3-D US and MRI, it came with a high correlation ($r = 0.79$). The high correlation indicates that a systematic bias was present in this study, which improved even further after re-processing the data with the new echo-canceling threshold amplitude. Similarly, a high correlation was also seen for DV estimates, which were less affected when re-processing the data. However, there was a poor correlation ($r = 0.43$) for volume flow estimates, which was exacerbated with the new echo-canceling filter parameter ($r = 0.31$), even though the underestimation was only -9%. These findings indicate that velocity estimates at the center of the vessel have a much higher accuracy than velocity estimates closer to the vessel boundaries. These results, moreover, address the necessity of designing the echo-canceling filter properly, such that

Table 2. Correlation statistics for MRI compared with 3-D US for both the original choice of echo-canceling filter and with the modified threshold value

| Variable | Stroke volume (mL/stroke) | | PSV (cm/s) | | DV (cm/s) | |
	MRI vs. 3-D US	MRI vs. 3-D US new filter	MRI vs. 3-D US	MRI vs. 3-D US new filter	MRI vs. 3-D US	MRI vs. 3-D US new filter
R	0.43	0.31	0.79	0.84	0.79	0.78
Mean difference	1.75	0.70	-23.76	-27.22	1.03	-0.75
Limits of agreement	2.89	2.90	33.30	21.60	4.94	6.00
p	<0.01	0.19	<0.01	<0.01	0.26	0.49

MRI = magnetic resonance imaging; 3-D US = 3-D ultrasound; 3-D US new filter = 3-D US with new echo-canceling filter; PSV = peak systolic velocity; DV = diastolic velocity.
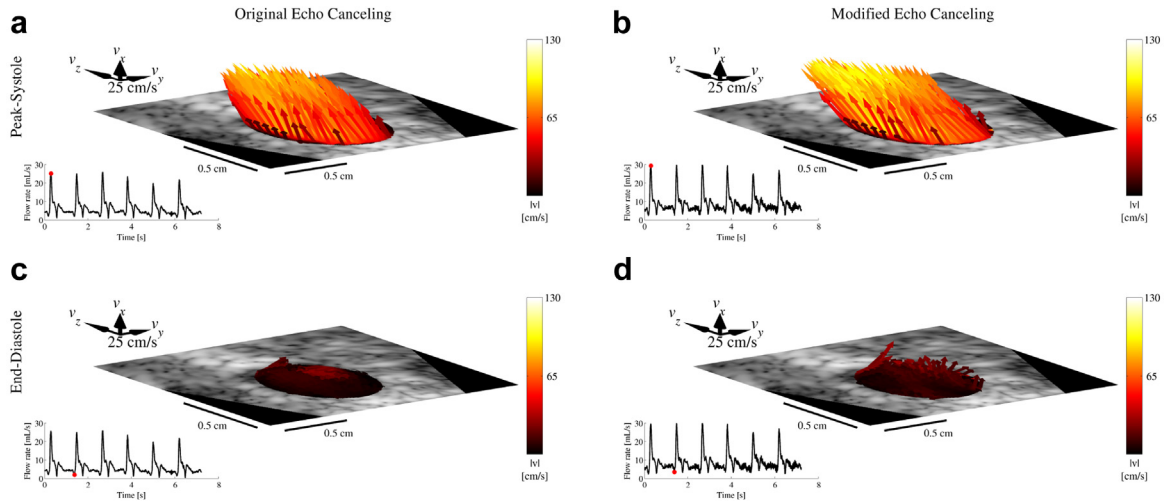
Fig. 3. Three-dimensional vector flow from the common carotid artery of volunteer 1 during peak systole (a,b) and end diastole (c,d). Left column: Values obtained with the original echo-canceling threshold. Right column: 3-D flow with the modified threshold. The *colored arrows* depict the direction of the flow and its magnitude. The scan was not performed exactly perpendicular to the vessel, which is revealed during peak systole, where a significant v_y velocity component is present. The graphs at the bottom left depict the flow rate at the time in the heart cycle indicated by the *red dot*.

clutter signal can be removed satisfactorily within the entire vessel so estimates close to the vessel boundary can be determined correctly.

The results indicated that compared with MRI, both SDUS and 3-D US generally overestimated PSV. This is in good agreement with the previously reported finding that compared with MRI, 1-D Doppler techniques overestimate peak velocities (Harloff et al. 2009; Karwatowski et al. 1995; Wetzel et al. 2007). One possible explanation for the overestimation found with SDUS could be errors arising from geometric spectral broadening (Hoskins et al. 1999). The difference in estimated peak velocities is expected to be due to the lower temporal and spatial resolution for MRI compared with US (Wetzel et al. 2007). Furthermore, MRI data are averaged from 210 heart cycles, which corresponds to low-pass filtering of the data. Contrarily, the 3-D US estimates were averaged from only 7.5 s of data, which translates to less than 10 cycles. Although variations in hemodynamics between the 3-D US and MRI examinations may partly explain the difference in estimated peak velocities and flow rates, it was not expected to be a major issue in this study, as the SDUS reference measurements of mean peak velocity were 100 ± 23 cm/s for 3-D US and 99 ± 28 cm/s for MRI.

In this study, a mask was drawn manually based on a B-mode image for each of the volunteers to segment the lumen. As the same mask was applied throughout the entire acquisition, expansion or contraction of the vessel during the cardiac cycle or displacement of the vessel caused by movement was not tracked. The lack of tracking of the vessel wall through time may cause an un-

derestimation of the flow rates. However, the effect of a static mask was not expected to have a significant impact on the peak velocities obtained with 3-D US, as this would require a relatively large displacement.

One source of error is the location of the scan plane. It could not be ensured that the velocity estimates were conducted at the exact same location for MRI and 3-D US. The scan plane for both imaging modalities was located approximately 2–3 cm upstream of the bifurcation for all volunteers, but their proximity to each other could not be determined. This source of error would only have a minor influence on the estimated peak velocities and would overall cancel out, as either of the two methods' scan planes could be located before or after the other.

CONCLUSIONS

This study indicates that compared with MRI, the proposed method for 3-D VFI overestimates PSV on average by 34%, but underestimates volume flow by 24%. However, the correlations were high for PSV ($r = 0.79$) and DV ($r = 0.79$). The overestimation was expected to be due to the higher temporal and spatial resolution. The study also indicated that the 3-D VFI method had a precision better than $\pm 10\%$ for both volume flow and PSV in all nine volunteers, but had a poor correlation of $r = 0.43$. In conclusion, the performance of the method is highly influenced by how well the stationary echo-canceling filter adapts to the present physiology. With a modified echo-canceling filter, the underestimation in volume flow was reduced to 9% with an overall improved SD, but with an even poorer correlation of $r = 0.31$.

REFERENCES

Alexandrov AV, Brodie DS, McLean A, Hamilton P, Murphy J, Burns PN. Correlation of peak systolic velocity and angiographic measurement of carotid stenosis revisited. Stroke 1997;28: 339–342.

Bland JM, Altman DG. Statistical methods for assessing agreement between two methods of clinical measurement. Lancet 1986;327: 307–310.

Bohs LN, Trahey GE. A novel method for angle independent ultrasonic imaging of blood flow and tissue motion. IEEE Trans Biomed Eng 1991;38:280–286.

Brandt AH, Jensen J, Hansen KL, Hansen PM, Lange T, Rix M, Jensen JA, Lönn L, Nielsen MB. Surveillance for hemodialysis access stenosis: Usefulness of ultrasound vector volume flow. J Vasc Access 2016;17:483–488.

Correia M, Provost J, Tanter M, Pernot M. 4D ultrafast ultrasound flow imaging: In vivo quantification of arterial volumetric flow rate in a single heartbeat. Phys Med Biol 2016;61:L48–L61.

Fadnes S, Ekroll IK, Nyrnes SA, Torp H, Løvstakken L. Robust angle-independent blood velocity estimation based on dual-angle plane wave imaging. IEEE Trans Ultrason Ferroelectr Freq Control 2015;62:1757–1767.

Food and Drug Administration. Information for manufacturers seeking marketing clearance of diagnostic ultrasound systems and transducers. Technical report. Center for Devices and Radiological Health, U.S. Food and Drug Administration; 2008.

Friemel BH, Bohs LN, Nightingale KR, Trahey GE. Wall filtering challenges in two-dimensional vector velocity estimation. Proc IEEE Int Ultrason Symp 1993;2:1031–1034.

Ge S, Bu L, Zhang H, Schelbert E, Disterhoft M, Li X, Li X, Sahn D, Stolpen A, Sonka M. A real-time 3-dimensional digital Doppler method for measurement of flow rate and volume through mitral valve in children: A validation study compared with magnetic resonance imaging. J Am Soc Echocardiogr 2005;18:1–7.

Hansen KL, Udesen J, Oddershede N, Henze L, Thomsen C, Jensen JA, Nielsen MB. In vivo comparison of three ultrasound vector velocity techniques to MR phase contrast angiography. Ultrasonics 2009;49: 659–667.

Hansen KL, Møller-Sørensen H, Kharghar J, Jensen MB, Lund JT, Pedersen MM, Olesen JB, Jensen JA, Nielsen MB. Vector flow imaging compared with conventional Doppler ultrasound and thermo-dilution for estimation of blood flow in the ascending aorta. Ultrason Imaging 2017;39:3–18.

Harloff A, Albrecht F, Spreer J, Stalder AF, Bock J, Frydrychowicz A, Schollhorn J, Hetzel A, Schumacher M, Hennig J, Markl M. 3D blood flow characteristics in the carotid artery bifurcation assessed by flow-sensitive 4D MRI at 3T. Magn Reson Med 2009;61:65–74.

Harloff A, Zech T, Wegent F, Strecker C, Weiller C, Markl M. Comparison of blood flow velocity quantification by 4D flow MR imaging with ultrasound at the carotid bifurcation. Am J Neuroradiol 2013; 34:1407–1413.

Higginbotham MB, Morris KG, Williams RS, McHale PA, Coleman RE, Cobb FR. Regulation of stroke volume during submaximal and maximal upright exercise in normal man. Circ Res 1986;58: 281–291.

Holbek S, Christiansen TL, Stuart MB, Beers C, Thomsen EV, Jensen JA. 3-D vector flow estimation with row-column addressed arrays. IEEE Trans Ultrason Ferroelectr Freq Control 2016;63: 1799–1814.

Holbek S, Ewertsen C, Bouzari H, Pihl MJ, Hansen KL, Stuart MB, Nielsen MB, Jensen JA. Ultrasonic 3-D vector flow method for quantitative in vivo peak velocity and flow rate estimation. IEEE Trans Ultrason Ferroelectr Freq Control 2017;64:544–554.

Hoskins P, Fish P, Pye S, Anderson T. Finite beam-width ray model for geometric spectral broadening. Ultrasound Med Biol 1999;25: 391–404.

Jensen JA. A new estimator for vector velocity estimation. IEEE Trans Ultrason Ferroelectr Freq Control 2001;48:886–894.

Jensen JA, Munk P. A new method for estimation of velocity vectors. IEEE Trans Ultrason Ferroelectr Freq Control 1998;45:837–851.

Jensen JA, Holten-Lund H, Nilsson RT, Hansen M, Larsen UD, Domsten RP, Tomov BG, Stuart MB, Nikolov SI, Pihl MJ, Du Y, Rasmussen JH, Rasmussen MF. Sarus: A synthetic aperture real-time ultrasound system. IEEE Trans Ultrason Ferroelectr Freq Control 2013;60:1838–1852.

Jensen J, Olesen JB, Stuart MB, Hansen PM, Nielsen MB, Jensen JA. Vector velocity volume flow estimation: Sources of error and corrections applied for arteriovenous fistulas. Ultrasonics 2016;70: 136–146.

Karwatowski SP, Brecker SJD, Yang GZ, Firmin DN, Sutton MSJ, Underwood SR. Mitral valve flow measured with cine MR velocity mapping in patients with ischemic heart disease: comparison with Doppler echocardiography. J Magn Reson Imaging 1995;5:89–92.

Lenge M, Ramalli A, Tortoli P, Cachard C, Liebgott H. Plane-wave transverse oscillation for high-frame-rate 2-D vector flow imaging. IEEE Trans Ultrason Ferroelectr Freq Control 2015;62:2126–2137.

Nikolov SI, Jensen JA. In-vivo synthetic aperture flow imaging in medical ultrasound. IEEE Trans Ultrason Ferroelectr Freq Control 2003; 50:848–856.

Phillips DJ, Powers JE, Blackshear WM, Bodily KC, Starkness DE, Baker DW. Detection of peripheral vascular disease using the duplex scanner III. Ultrasound Med Biol 1980;6:205–218.

Picot PA, Embree PM. Quantitative volume flow estimation using velocity profiles. IEEE Trans Ultrason Ferroelectr Freq Control 1994;41: 340–345.

Pihl MJ, Jensen JA. A transverse oscillation approach for estimation of three-dimensional velocity vectors: Part I. Concept and simulation study. IEEE Trans Ultrason Ferroelectr Freq Control 2014;61: 1599–1607.

Pihl MJ, Stuart MB, Tomov BG, Rasmussen MF, Jensen JA. A transverse oscillation approach for estimation of three-dimensional velocity vectors: Part II. Experimental validation. IEEE Trans Ultrason Ferroelectr Freq Control 2014;51:1608–1618.

Provost J, Papadacci C, Arango JE, Imbault M, Fink M, Gennisson JL, Tanter M, Pernot M. 3-D ultrafast ultrasound imaging in vivo. Phys Med Biol 2014;59:L1–L13.

Struijk P, Stewart P, Fernando K, Mathews V, Loupas T, Steegers E, Wladimiroff J. Wall shear stress and related hemodynamic parameters in the fetal descending aorta derived from color Doppler velocity profiles. Ultrasound Med Biol 2005;31:1441–1450.

Udesen J, Gran F, Hansen KL, Jensen JA, Thomsen C, Nielsen MB. High frame-rate blood vector velocity imaging using plane waves: Simulations and preliminary experiments. IEEE Trans Ultrason Ferroelectr Freq Control 2008;55:1729–1743.

Villagomez-Hoyos CA. Synthetic aperture vector flow imaging. Ph.D. thesis. Technical University of Denmark. Available at: http://findit.dtu.dk/en/catalog/2347162876. 2016. Accessed June 2016.

Villagomez-Hoyos CA, Holbek S, Stuart MB, Jensen JA. High frame rate synthetic aperture 3D vector flow imaging. Proc IEEE Int Ultrason Symp 2016a;1–4.

Villagomez-Hoyos CA, Stuart MB, Hansen KL, Nielsen MB, Jensen JA. Accurate angle estimator for high frame rate 2-D vector flow imaging. IEEE Trans Ultrason Ferroelectr Freq Control 2016b;63: 842–853.

Wetzel S, Meckel S, Frydrychowicz A, Bonati L, Radue EW, Scheffler K, Hennig J, Markl M. In vivo assessment and visualization of intracranial arterial hemodynamics with flow-sensitized 4D MR imaging at 3T. Am J Neuroradiol 2007;28:433–438.

Whittier WL. Surveillance of hemodialysis vascular access. Semin Interv Radiol 2009;26:130–138.

Wiese P, Nonnast-Daniel B. Colour Doppler ultrasound in dialysis access. Nephrol Dial Transpl 2004;19:1956–1963.

Wigen M, Løvstakken L. In vivo three-dimensional intra-cardiac vector flow imaging using a 2D matrix array transducer. Proc IEEE Int Ultrason Symp 2016;1–4.

Yiu BY, Lai SS, Yu AC. Vector projectile imaging: time-resolved dynamic visualization of complex flow patterns. Ultrasound Med Biol 2014;40:2295–2309.